

A Cross-Benchmarking and Validation Initiative for Tokamak 3D Equilibrium Calculations

A. Reiman¹, A. Turnbull², T. Evans², N. Ferraro², E. Lazarus³, J. Breslau¹, A. Cerfon⁴,
C.S. Chang¹, R. Hager¹, J. King³, M. Lanctot², S. Lazerson¹, Y. Liu⁵, G. McFadden⁶,
D. Monticello¹, R. Nazikian¹, J.K. Park¹, C. Sovinec⁷, Y. Suzuki⁸, P. Zhu⁷

¹*Princeton Plasma Physics Laboratory, Princeton, NJ 08543 USA*

²*General Atomics, P.O. Box 85608, San Diego, California 92186-5608, USA*

³*Oak Ridge National Laboratory, Oak Ridge, TN, USA*

⁴*New York University, New York, NY, USA*

⁵*EURATOM/CCFE Fusion Association, Culham Science Centre, Abingdon, Oxon, UK*

⁶*National Institute of Standards and Technology, Gaithersburg, MD, USA*

⁷*University of Wisconsin, Madison, WI, USA*

⁸*National Institute for Fusion Science, Kyoto, Japan*

We are pursuing a cross-benchmarking and validation initiative for tokamak 3D equilibrium calculations, with 11 codes participating: the linearized tokamak equilibrium codes IPEC[1] and MARS-F[2], the time-dependent extended MHD codes M3D-C1[3], M3D[4], and NIMROD[5], the gyrokinetic code XGC[6], as well as the stellarator equilibrium codes VMEC[7], NSTAB[8], PIES[9], HINT2[10] and SPEC[11]. Dedicated experiments for the purpose of generating data for validation have been done on the DIII-D tokamak. The data will allow us to do validation simultaneously with cross-benchmarking. Cross-benchmarking calculations have been finding a disagreement between the VMEC stellarator equilibrium code and tokamak linearized 3D equilibrium codes. Investigation of the source of the disagreement has led to new insights into the domain of validity of these codes. Solutions from additional codes provide further insight into the source of the disagreement. In Ref 12, comparisons of linear and nonlinear plasma response models are discussed in terms of differences between dynamic evolution and perturbed equilibrium calculations. (Note that the magnetic field used there for the VMEC calculations was different from that used for the linearized calculations.)

Both stellarator and tokamak equilibrium codes are participating in our initiative. Some of the stellarator codes assume “stellarator symmetry”, which is a symmetry of the magnetic field with respect to combined reflection in the poloidal and toroidal angles. On the other hand, some of the tokamak equilibrium codes are perturbative, assuming that the nonaxisymmetric component of the magnetic field is small compared to the axisymmetric component. We are working with equilibria that have both of these properties, to allow us to do cross-benchmarking between stellarator and tokamak codes. Our initial calculations have focused on DIII-D shot number 142603, which was part of a campaign to study ELM suppression using externally imposed nonaxisymmetric fields

Fig. 1 shows the radial displacement of the $q = 8.5/3$ surface as a function of the poloidal angle, relative to the corresponding axisymmetric equilibrium solution, as calculated by VMEC, IPEC and MARS-F. There is a significant disagreement between the VMEC solution and the solutions from the linearized equilibrium codes on the inboard side. We have identified two sources of disagreement between the codes. One source of disagreement has emerged from a study of the solutions for simple model equilibria. The equilibria have large aspect ratio and a circular boundary perturbed by a single harmonic. Fig. 2 shows IPEC solutions for three such equilibria and also the corresponding solutions for a perturbed circular cylinder. The IPEC solutions are close to those for a cylinder. There is an $n = 1, m = 2$ surface in the plasma, and the normal displacement in the cylindrical solution goes to zero inside that surface. The IPEC

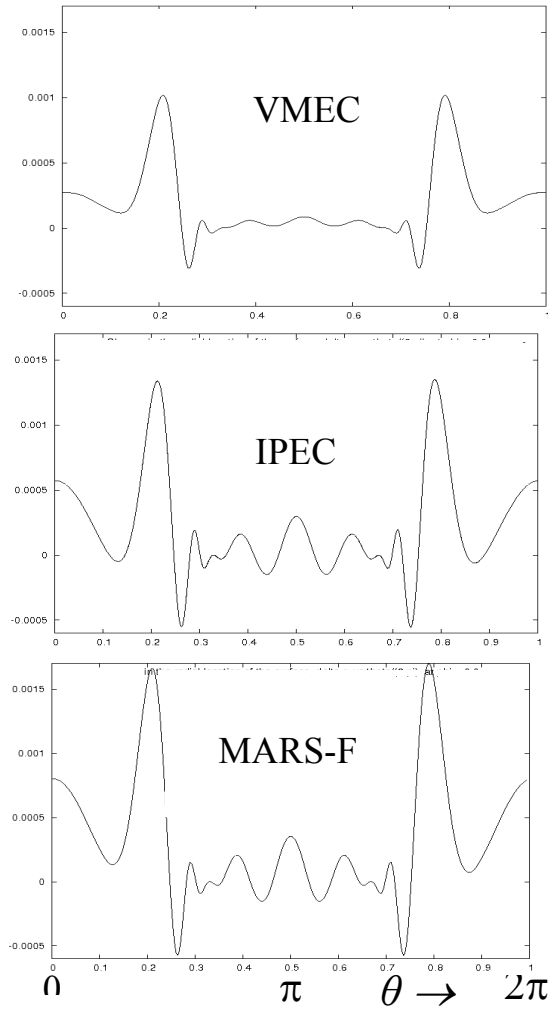


Fig. 1. Perturbation amplitude (change in the radial location of the $q = 8.5/3$ surface) at $\phi = 0$ as a function of the poloidal angle, as calculated by VMEC, IPEC and MARS-F. $\theta = 0$ corresponds to the outboard midplane and $\theta = \pi$ to the inboard midplane. (Data from E. Lazarus, J-K Park, and A. Turnbull.)

2 component of the current density is becoming resolution, but even with 1600 radial grid surfaces the VMEC solution is not close to a step function. (A similar VMEC study, with similar results, was done by Monticello *et al.*[13])

A second source of disagreement between VMEC and the linearized codes is the linearization itself. The linear approximation is valid only when the amplitude of the perturbation is sufficiently small. IPEC assumes good surfaces. When the amplitude of the perturbation is sufficiently large, the perturbed flux surfaces overlap, signaling a breakdown of the linear approximation. Figure 5 shows an evaluation of the overlap criterion for an equilibrium calculated by the linearized M3D-C1 code for shot 142603. Roughly everything outside of the $q = 3.5$ surface satisfies the overlap condition, despite the fact that the perturbation amplitude is $\delta B / B \approx 10^{-3}$. The overlap condition is also satisfied in the neighbourhood of the rational surfaces. Although the assumption of good surfaces breaks down in the overlap region, it is still possible to calculate a perturbed magnetic field in that region. The field lines are stochastic. It remains to determine whether the magnetic field calculated in this way gives a useful approximation to the self-consistent field.

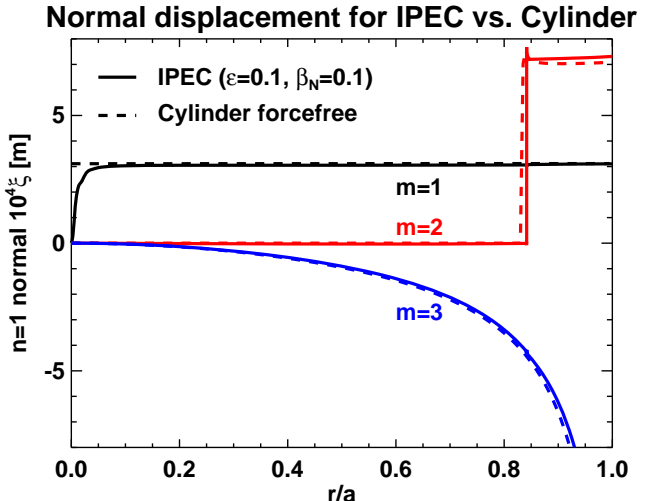


Fig. 2. IPEC solutions for three equilibria having $R/a = 10$ and a circular boundary perturbed by a single harmonic having toroidal mode number $n = 1$. For comparison, the dashed lines show the corresponding analytic solutions for a perturbed cylinder. (Figure from J.K. Park.)

solution near the $q = 2$ surface is approximately a step function, and there is a localized current near the rational surface that is associated with the large radial derivative of the displacement.

Fig. 3 shows a set of VMEC solutions for $R/a = 100$, a circular boundary perturbed by a single, $n = 1$, $m = 2$ Fourier harmonic with magnitude 10^{-6} , and various numbers of radial grid surfaces. (The amplitude of the perturbation is plotted relative to its value on the boundary.) It is plausible that the solutions will converge to an approximate step function as the number of radial grid surfaces is further increased, but even with 1600 radial grid surfaces the VMEC solution is not close to a step function. The corresponding component of the current density is shown in Fig. 4. The $n = 1$, $m =$

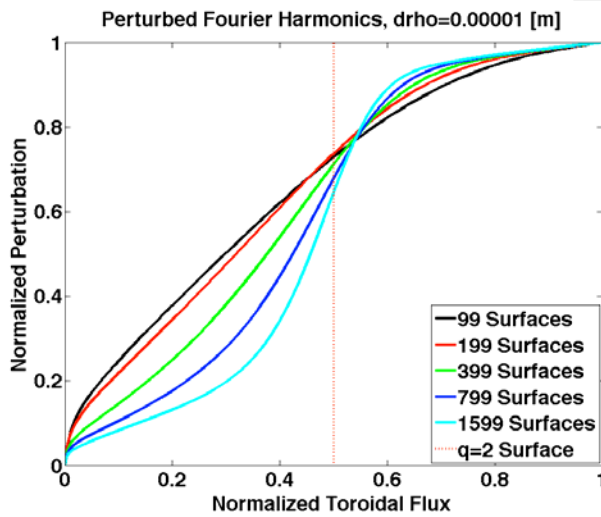


Fig. 3. VMEC solutions with $R/a=100$, a perturbed circular boundary, and various numbers of radial grid surfaces. (Figure from S. Lazerson.)

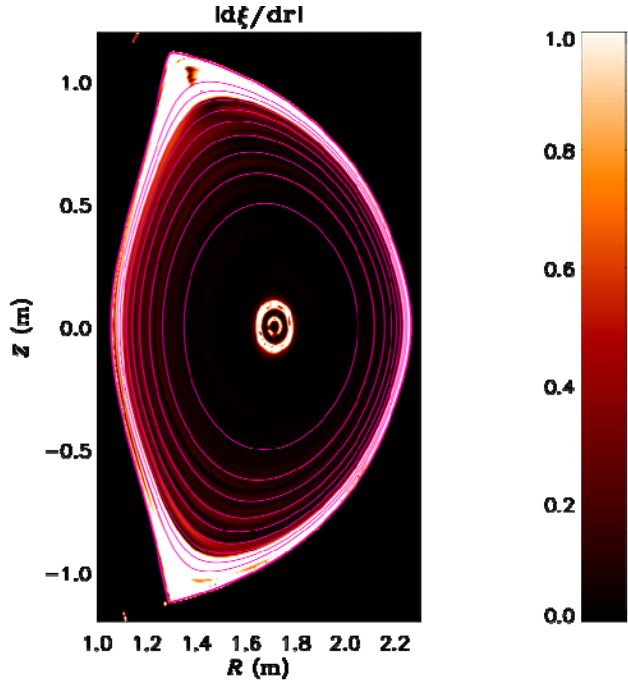


Fig. 5. Evaluation of overlap condition for an equilibrium calculated by the linearized M3D-C1 code for shot 142603. (Figure from N. Ferraro.)

to a solution of the linearized equilibrium equations, the pink line to a nonlinear solution at $t = 16 \mu\text{s}$, and the blue line to a nonlinear solution at $t = 260 \mu\text{s}$. Despite the breakdown of the linear approximation in a substantial region near the plasma boundary, the linear and nonlinear solutions are approximately equal. This suggests that the difference between the linearized codes and VMEC is probably not caused by the breakdown of the linear approximation. A more likely explanation is the difficulty that VMEC has in handling localized currents at rational surfaces.

N. Ferraro has also produced M3D-C1 solutions for rotating and nonrotating plasmas. Plasma rotation is known to drive screening currents at rational surfaces. The nonrotating plasma gives an equilibrium solution with a small perturbation amplitude on the inboard side.

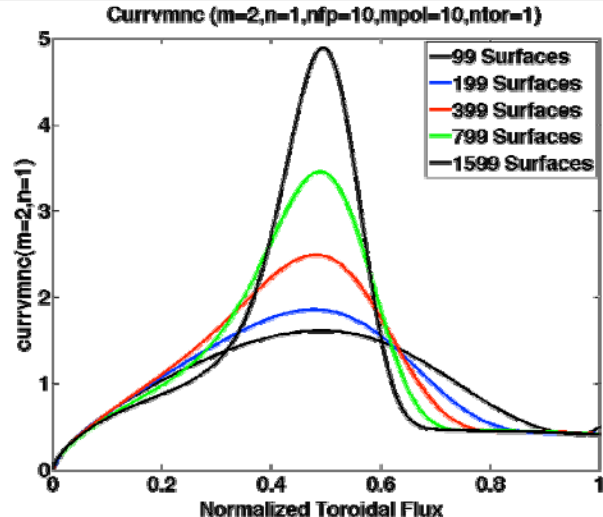


Fig. 4. Magnitude of the $n = 1$, $m = 2$ component of the current for the equilibrium solutions of Fig. 3. (Fig. from S. Lazerson.)

Boozer and Pomphrey have looked at the consequences of the breakdown of the linear approximation in the neighborhood of rational surfaces.[14] The localized current in the linear solution does not entirely eliminate island formation at the rational surface. A small island remains, filling the region where the linear approximation breaks down. The residual island is much smaller than the island that would appear in the absence of the localized current.

The $q=8.5/3$ surface is stochasticized in the equilibrium solution produced by the HINT2 code (Y. Suzuki), and it is also broken in the nonlinear M3D-C1 equilibrium solution (N. Ferraro).

Fig. 6 is an overlay of three Poincare plots for the perturbed $q=2.42$ flux surface in M3D-C1 equilibrium solutions, with the perturbation scaled up by a factor of 20 to make it visible. The green line corresponds to a linearized solution, the blue line to a nonlinear solution at $t = 16 \mu\text{s}$, and the pink line to a nonlinear solution at $t = 260 \mu\text{s}$. Despite the breakdown of the linear approximation in a substantial region near the plasma boundary, the linear and nonlinear solutions are approximately equal. This suggests that the difference between the linearized codes and VMEC is probably not caused by the breakdown of the linear approximation. A more likely explanation is the difficulty that VMEC has in handling localized currents at rational surfaces.

Fig. 6 is an overlay of three Poincare plots for the perturbed $q=2.42$ flux surface in M3D-C1 equilibrium solutions, with the perturbation scaled up by a factor of 20 to make it visible. The green line corresponds to a linearized solution, the blue line to a nonlinear solution at $t = 16 \mu\text{s}$, and the pink line to a nonlinear solution at $t = 260 \mu\text{s}$. Despite the breakdown of the linear approximation in a substantial region near the plasma boundary, the linear and nonlinear solutions are approximately equal. This suggests that the difference between the linearized codes and VMEC is probably not caused by the breakdown of the linear approximation. A more likely explanation is the difficulty that VMEC has in handling localized currents at rational surfaces.

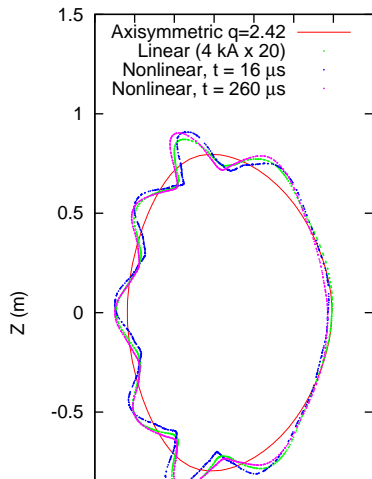


Fig. 6. Overlay of three Poincare plots for the perturbed $q=2.42$ flux surface in M3D-C1 equilibrium solutions, with the perturbation scaled up by a factor of 80. (Ferraro)

A solution with an imposed rotation frequency equal to that observed in the experiment displays a larger perturbation amplitude on the inboard side. This provides further evidence that the disagreement between VMEC and the linear codes can arise from the absence of localized screening currents in VMEC.

McFadden, Cerfon and Lazerson have produced an equilibrium solution for shot 142603 using the NSTAB code. NSTAB is similar to VMEC, in that it assumes good surfaces, but it does not have a free boundary capability. It is believed that NSTAB handles localized currents at rational surfaces more accurately than VMEC. NSTAB was used to do a fixed boundary calculation, with the VMEC plasma boundary shape imposed. Nevertheless, the NSTAB solution is intermediate between that of VMEC and the linear codes, showing a larger perturbation amplitude on the inboard side than VMEC. This provides further evidence that the disagreement between VMEC and the linear codes arises from the absence of localized screening currents in VMEC.

The evidence suggests that the VMEC solution for DIII-D shot 142603 differs from the solutions of the linearized equilibrium codes because of the absence of localized screening currents in VMEC. The question remains whether such currents actually exist in experiments. A series of experiments has been done on DIII-D, including important new diagnostic capabilities, in part to answer that question. The diagnostics included more than 100 new magnetic field sensors positioned on the high and low field sides of the tokamak. A set of shots and time slices are being selected for further analysis, and the data will be used for validating 3D equilibrium calculations.

Acknowledgement: This work was supported in part by the U.S. Department of Energy under contracts DE-AC02-09CH11466, DE-FC02-04E854698, DE-FG02-95E854309 and DE-AC05-000R22725.

References

- [1] J.-K. Park, A. H. Boozer, and A. H. Glasser, Phys. Plasmas **14**, 052110 (2007).
- [2] Y. Q. Liu, A. Bondeson, C. M. Fransson, B. Lennartson, C. Breitholtz, Phys. Plasmas **7**, 3681 (2000).
- [3] N. M. Ferraro, S. C. Jardin, and P. B. Snyder, Phys. Plasmas **17**, 102508 (2010).
- [4] W. Park, E. V. Belova, G. Y. Fu, X. Z. Tang, H. R. Strauss and L. E. Sugiyama, Phys. Plasmas **6**, 1796 (1999).
- [5] A. H. Glasser, C. R. Sovinec, R. A. Nebel, T. A. Gianakon, S. J. Plimpton, M. S. Chu, D. D. Schnack, and the NIMROD Team, Plasma Phys. Controlled Fusion **41**, A747 (1999).
- [6] C. S. Chang and S. Ku Phys. Plasmas **11**, 5626 (2004); J. Phys.: Conf. Ser. **46**, 87 (2006).
- [7] S. P. Hirshman and D. K. Lee, Comput. Phys. Commun. **39**, 161 _1986_.
- [8] M. Taylor, J. Comput. Phys., **110**, 407 (1994).
- [9] A. H. Reiman and H. Greenside, Comput. Phys. Commun. **43**, 157 (1986); D. Monticello, A. Reiman and D. Raburn, Bull. Am. Phys. Soc. **58**, 258 (2013).
- [10] Y. Suzuki, N. Nakajima, K. Watanabe, Y. Nakamura and T. Hayashi, Nucl. Fusion **46**, L19–L24 (2006).
- [11] S. R. Hudson, R. L. Dewar, G. Dennis, M. J. Hole, M. McGann, G. von Nessi, and S. Lazerson, Phys. Plasmas **19**, 112502 (2012).
- [12] A. Turnbull et al, Phys. Plasmas **20**, 056114 (2013).
- [13] D. Monticello *et al*, US/Japan JIFT workshop, Princeton, NJ, December 2002, <https://docs.google.com/file/d/0B3SxUyX3eGoWWHbKxTVXNGNGs/edit>
- [14] A. Boozer and N. Pomphrey, Phys. Plasmas **17**, 110707 (2010).